scientific reports

Check for updates

OPEN

Long-term competition experiments reveal limited adaptive evolution in human cell lines

Elżbieta Speina[1,3]✉, Agnieszka Tupalska[1,3], Iwona Grądzka[2], Kamila Kłosowska-Kosicka[1], Jacek Bardowski[1], Roman J. Szczesny[1] & Szymon Kaczanowski[1]✉

Cancer progression is driven by somatic evolution, where mutations and selection generate more adapted clones. However, it remains unclear whether human cells continue to evolve under stable laboratory conditions or instead reach a near-optimal state. We addressed this using two human cell lines, HeLa and 293, with isogenic subpopulations differing only by a fitness-neutral marker (inducible GFP expression). Mixed GFP⁺ and GFP⁻ populations were co-cultured for 12 months under constant conditions, with competition assays performed with or without periodic GFP induction and sorting. In a parallel experiment inspired by Velicer's microbial studies, GFP⁺ cells were exposed to independently cultured, non-evolving GFP⁻ populations to test whether competitively advantageous variants could emerge when competitors could not respond. Initially, we observed patterns consistent with genetic drift, followed by a gradual expansion of GFP⁻ cells. After 4–6 months, a likely beneficial mutation in the GFP⁺ 293 population reversed this trend, whereas GFP⁻ HeLa cells retained their advantage. Fitness differences were small, and observed dynamics were consistent with weak selection. These results suggest that long-term cultured human cells evolve slowly without rapid clonal expansion.

Keywords Somatic evolution, Adaptive evolution, Clonal dynamics, GFP marker, *In vitro* evolution, Selection experiments

Over a century ago, Theodor Boveri[1] observed that the chromosomal patterns of cancer cells differ from those of normal cells and proposed that genetic instability underlies malignant transformation. In 1976, Peter Nowell described cancer as an evolutionary process driven by stepwise somatic mutations and subclonal selection[2], a concept that is now strongly supported by genomic studies [3–5]. Drug resistance in cancer cells develops through evolutionary mechanisms analogous to the selection of resistant bacterial mutants[6,7].

Cancer is characterized by extensive genetic heterogeneity[8,9] and the accumulation of numerous oncogenic mutations[7,10]. During neoplastic transformation, suppression of apoptosis represents an essential step [11,12], and tumor progression is associated with profound phenotypic changes. Cancer cells display dysregulated cell-cycle control[13], genetic instability[14–16], and a metabolic shift from oxidative respiration to glycolysis, as first noted by Otto Warburg in his classical observations[17]. Cancer progression provides a vivid example of somatic evolution, in which mutation and selection act together to shape cellular phenotypes by expanding higher-fitness subclones. In this process, certain subclones acquire growth advantages, enabling them to invade and dominate the population. Metastasis can be viewed as an advanced manifestation of this evolutionary process, where cancer cells adapt to novel microenvironments and overcome diverse physiological barriers. Although the selective landscape changes across stages, the underlying principle remains the same: continuous selection for variants with improved fitness in a given context[18]. Many tumors also harbor cancer stem cells with self-renewing and tumor-initiating potential[19].

[1]Institute of Biochemistry and Biophysics, Polish Academy of Sciences, Pawińskiego 5a, 02-106, Warsaw, Poland. [2]Institute of Nuclear Chemistry and Technology, Centre for Radiobiology and Biological Dosimetry, Dorodna 16, 03-195 Warsaw, Poland. [3]Elżbieta Speina and Agnieszka Tupalska contributed equally to this work. ✉email: elasp@ibb.waw.pl; szymon@ibb.waw.pl

The pathological somatic evolution of human cells into malignant cells results in dramatic phenotypic changes, including metabolic reprogramming. Cancer has also been discussed as an example of competitively advantageous cellular behaviors[20]. In this context, such behaviors refer to the breakdown of cooperative rules, genetically encoded or behavioral, that confer a fitness advantage to particular clones while being detrimental to the surrounding cell population. The emergence of such strategies is not unique to cancer; it has also been observed in microorganisms. For example, *Myxococcus xanthus* forms multicellular fruiting bodies under starvation, in which a fraction of the cells differentiates into stress-resistant spores. Certain cells preferentially differentiate into spores without contributing to the communal cost of fruiting body formation[21]. Malignant transformation has been proposed to represent a reversion from the differentiated state of multicellular organisms to an ancestral, unicellular-like phenotype[7,22]. During somatic evolution, cancer cells develop diverse strategies to exploit host tissues[23] and may even induce apoptosis in surrounding normal cells[24,25]. Thus, cancer cells can be viewed as unicellular parasites that evolved from human cells, although cooperative behaviors among them have also been documented[26]. Under specific experimental conditions, somatic evolution may generate cultures resembling free-living, non-parasitic unicellular organisms[27]. However, even such unicellular-like cells retain active intercellular communication and typical mechanisms of multicellular cooperation. For instance, tumor necrosis factor (TNF)-related apoptosis-inducing ligand (TRAIL) can induce apoptosis in HeLa cells[28–30].

Model cell lines such as HeLa and 293 have been cultured in the laboratory for decades, providing valuable systems for studying cellular adaptation and somatic evolution. Cancer cell lines are widely used as experimental models of rapid adaptation, particularly in the context of drug resistance and other strong selective pressures, yet much less is known about their evolutionary dynamics during prolonged maintenance in stable laboratory environments[31–33]. Although these cells are known to undergo rapid adaptive evolution under altered conditions, it remains unclear whether they have reached a near-optimal state of adaptation after prolonged culture in stable environments. Since long-term evolution experiments performed *in vitro* primarily reflect adaptation to the culture setting itself, their direct clinical relevance is limited. Nevertheless, determining whether long-term cultured cell lines continue to evolve adaptively or instead approach an evolutionary equilibrium under constant, non-selective conditions provides an important baseline reference for interpreting evolutionary responses observed under clinically relevant stressors. Accordingly, it remains unclear whether, after prolonged culture under stable conditions, these cells have reached a near-optimal adaptive state in which further evolution is primarily limited to genetic drift. Classical long-term evolution experiments, such as Lenski's study with *Escherichia coli*, demonstrate that beneficial mutations can continue to arise even after tens of thousands of generations[34–38]. We hypothesized that, despite being widely considered evolutionarily stable, long-term cultured mammalian cell lines may still retain latent adaptive potential, enabling the emergence of higher-fitness variants even under constant laboratory conditions. Although this hypothesis may seem intuitively apparent, given the long-term maintenance and presumed adaptation of immortalized cell lines, it has not been experimentally verified. Therefore, our study aimed to empirically assess whether human cell lines that have been cultured for decades, such as HeLa and 293, indeed represent evolutionarily saturated systems or whether spontaneous adaptive divergence can still occur in the absence of environmental pressures. HeLa cells, derived from cervical carcinoma in 1951[39], likely originated following the integration of human papillomavirus type 18 (HPV-18) into chromosome 8[40,41]. They are hypertriploid and carry characteristic clonal chromosomal abnormalities known as the HeLa signature chromosomes[42]. Cytogenetic and genomic analyses indicate that HeLa cells exhibit a largely conserved genomic architecture across passages, with comparatively few new point mutations arising after early passages[40,43]. The 293 cell line, derived from human embryonic kidney cells, was established in 1973 following the integration of adenovirus 5 DNA into chromosome 15[44]. Like HeLa cells, 293 cells are pseudo-triploid and immortalized through viral integration. While phenotypic variation can be induced in both 293[33] and HeLa cells[31,32,45] through artificial selection, their prolonged maintenance under standard culture conditions may constrain further adaptive change. Consistent with this view, a recent study demonstrated a substantial genetic load in HeLa cells, contributing to measurable fitness diversity within populations[46]. To investigate whether long-term cultured human cells continue to evolve adaptively or can give rise to more competitive phenotypes under constant laboratory conditions, we performed long-term competition experiments using isogenic GFP^+ and GFP^- subpopulations of HeLa and 293 cells. GFP expression was regulated by a tetracycline-inducible system, enabling controlled induction without introducing confounding genetic differences. By monitoring temporal changes in population ratios and growth kinetics under non-induced, continuously induced, and transiently induced conditions, we assessed whether sustained fitness divergence emerges during extended culture. Our results indicate that both HeLa and 293 cell lines display remarkable evolutionary persistence under these stable conditions, with only very slow evolutionary change.

Methods

General description of the methodology

In principle, we expanded the concepts of Kishony's experiments[47] to human cell systems. In our study, isogenic HeLa cancer cells and immortalized 293 cells were transfected with tetracycline-inducible constructs encoding either the GFP gene (to generate "green" GFP^+ cells) or identical constructs lacking GFP (to generate "white" GFP^- cells). All cells were co-transfected with a hygromycin-resistance gene, and hygromycin was included in the culture medium throughout the experiment to prevent loss of the transgene. At the beginning of each cycle, sorted GFP^+ cells were mixed with freshly prepared GFP^- cells at an approximately 1:1 ratio (50% GFP^+ / 50% GFP^-). Therefore, transient increases in GFP^+ frequency immediately after sorting reflect enrichment of GFP^+ cells during the sorting step and the subsequent reset of starting proportions at the beginning of each cycle. Because small fitness differences may not be detectable in short-term assays, we used long-term serial passaging competition experiments as a sensitive cumulative readout of marker-associated fitness costs. Under this design, even weak persistent growth disadvantages are expected to accumulate over passages and

produce directional shifts in population ratios. Initial results indicated that GFP⁻ cells had a selective advantage. However, approximately six months later, in the 293 cell population, a putative beneficial mutation appeared in the GFP⁺ subpopulation, conferring a selection advantage in these cells. Significantly, the GFP gene was not induced during this phase of the experiment. We also examined whether beneficial mutations could be selected more rapidly, following the conceptual framework established by Velicer and colleagues. In their study, the social bacterium *Myxococcus xanthus* evolved through repeated encounters with a non-evolving strain that avoided the cost of cooperative behavior, eventually gaining competitive superiority and suppressing the competing population[48]. Such an approach can promote the selection of outcompeting cells in an evolutionary arms race between competing populations. In such a scenario, competing cells would evolve strategies that confer a fitness advantage over rivals, while simultaneously developing evolutionary responses to their rivals' strategies. Analogously, in our experiments, GFP⁺ cells were repeatedly exposed to non-evolving GFP⁻ cells. Every four weeks, tetracycline was added to induce GFP expression, followed by sorting of the cell populations. The results were similar to those observed in the experiment without sorting. Notably, when competing against non-evolving GFP⁻ HeLa cells, the evolving GFP⁺ population tended to be outcompeted.

Statistical analysis

The probability of fixation (mutant expansions/selective sweeps) in this type of evolutionary experiment was described in a theoretical study by Wahl and colleagues[49]. Their model estimates the probability that a beneficial mutation becomes fixed in a population undergoing periodic bottlenecks, as typically observed in laboratory evolution studies. In such experiments, whether involving bacteria, phages, or human cell cultures, a small subset of individuals is transferred to a new flask at each passage, creating a serial dilution regime. Under these conditions, the probability of fixation U(s) of the beneficial clone with a selective advantage can be approximated by the equation: $U(s) \approx 2sD(\ln D)^2$, where D represents the dilution rate. The highest probability of a selective sweep by new mutants occurs at a dilution rate of 1/10, which we applied in our experiment, and it was approximately equal to s. The probability that a new beneficial mutation arises in a population can be assessed either through multiple parallel replicate experiments or a single long-term evolution experiment. In practice, a single extended experiment is commonly used to detect beneficial mutations, as such events typically require considerable time to appear (see, for example, the study of Burch and Chao[50]). Additionally, we simulated fitness-neutral evolution in our experimental system using the R script provided in Fig. S1 (Supplementary Information). Simulations were initiated with 10,000 GFP⁺ and 10,000 GFP⁻ cells. During each simulated experiment, all cells underwent four rounds of division, resulting in a 16-fold increase in the number of both GFP⁺ and GFP⁻ cells ($2^4 = 16$). Four rounds of division were chosen to approximate the effective population expansion occurring between routine passaging steps in our experimental culture protocol. Subsequently, 10,000 cells were randomly sampled, and the process was repeated iteratively.

Cell culture

HeLa Flp-In T-REx (a kind gift from Matthias Hentze)[51] and 293 Flp-In T-REx cells (R78007, ThermoFisher Scientific, Waltham, MA, USA) were cultured in DMEM (Cytiva – HyClone, Logan, UT, USA), supplemented with 10% fetal bovine serum (FBS, ThermoFisher Scientific) and hygromycin (InvivoGen, San Diego, CA, USA) in a humidified incubator at 37° C with 5% CO_2. Cell lines expressing GFP (GFP⁺) were mixed with cells not expressing GFP (GFP⁻) at a 1:1 ratio at the beginning of the experiment and after each sorting. Cells were cultured in 75 cm^2 flasks at a density of 1 x 10^6 cells/flask for HeLa and 1.5 x 10^6 cells/flask for 293 cell lines, respectively.

Plasmids and establishment of stable cell lines

HeLa Flp-In T-REx and 293 Flp-In T-REx cells were transfected with either pKK-NoTag (pRS938; Addgene, Watertown, MA; ID 105767) or pKK-TEV-EGFP (pRS942, Addgene; ID 105793) plasmids using the standard Flp-In recombination system and selected under hygromycin resistance, as described in detail elsewhere[52]. Both plasmids, including their complete maps and nucleotide sequences, are publicly available through the Addgene repository (https://www.addgene.org). A schematic representation of the genetic constructs used to generate the GFP⁺ (pRS942, Addgene ID 105793) and GFP⁻ (pRS938, Addgene ID 105767) cell lines is provided in Fig. S2 (Supplementary Information).

Proliferation rate and statistical analysis

Cells were seeded at a density of 5×10^5 cells/dish in 10 cm Petri dishes and passaged twice weekly. After 2 weeks of culture with or without tetracycline (100 ng/mL), cells were reseeded onto 6 cm Petri dishes at a density of 2.5×10^5 cells/dish and treated with tetracycline (100 ng/mL) as indicated for the experimental group. Cell proliferation was assessed for GFP⁻ and GFP⁺ HeLa and 293 cell lines under three experimental conditions: non-induced, continuously tetracycline-induced, and pulse-induced (24 h exposure to tetracycline). For each condition, the number of viable cells was determined at 24, 48, 72, and 96 h by direct counting using a Neubauer chamber under a light microscope.

To determine growth rates, cell numbers were log-transformed and plotted as ln(cell number) versus time. The specific growth rate (μ, h^{-1}) was calculated for each biological replicate as the slope of the linear regression fitted to the exponential growth phase using GraphPad Prism (v. 9). Mean μ values from at least three independent biological replicates were compared between GFP⁻ and GFP⁺ cells using a two-tailed Student's *t*-test. When multiple induction conditions were analyzed simultaneously, a one-way ANOVA followed by Tukey's post hoc test was used. All statistical analyses were performed using STATISTICA software (v. 6). Differences were considered statistically significant at $p < 0.05$. No significant differences in proliferation rates were observed between GFP⁻ and GFP⁺ cells under any of the tested conditions.

Fluorescence-activated cell sorting

Fluorescence-activated cell sorting (FACS) was used to physically separate GFP⁺ and GFP⁻ subpopulations and to monitor the stability of GFP expression during long-term co-culture and induction experiments. The procedure was not intended to impose selective pressure but rather to verify whether repeated GFP induction and sorting could affect population structure or marker stability.

Cells were harvested after trypsin-EDTA treatment, centrifuged (125 × *g*, 5 min), and resuspended in culture medium containing 2% FBS. Cell sorting was performed using a FACSAria III flow cytometer (BD Biosciences, NJ, USA) with BD FACS Diva v. 8.0.1 software. GFP⁻ cells were used to set FSC-A and SSC-A parameters, and aggregates were excluded based on SSC-A/SSC-H gating. GFP⁺ cells were then physically separated from mixed populations and collected into tubes containing complete medium prewarmed to 37 °C. The purity of sorted GFP⁺ and GFP⁻ fractions consistently exceeded 90%, as confirmed by re-analysis. The sorted samples were subsequently used in competition assays to assess population ratios and confirm that GFP expression and sorting did not alter cell growth dynamics or competitive behavior.

In the Velicer-type competition assay, each experimental cycle corresponded to a four-week co-culture period (~28 generations), during which GFP⁺ cells were maintained in continuous interaction with independently propagated GFP⁻ populations. At the end of each four-week cycle, mixed cultures were analyzed by flow cytometry to determine the relative proportions of GFP⁺ and GFP⁻ cells. Subsequently, GFP⁺ cells were isolated by FACS and then remixed with freshly prepared GFP⁻ cells in a defined 1:1 ratio to initiate the next competition cycle. This procedure ensured that GFP⁻ cells did not co-evolve with GFP⁺ cells and that both subpopulations were initiated in each cycle under standardized conditions. The temporary increase in the GFP⁺ fraction immediately after sorting reflected the initial enrichment of the GFP⁺ subpopulation by the sorting step itself. Subsequent measurements during each four-week co-culture phase represented genuine changes in population structure driven by competitive interactions rather than by sorting bias. This cyclic procedure was repeated for 12 consecutive cycles (corresponding to approximately 12 months of total culture). The purity of sorted GFP⁺ fractions was confirmed by post-sorting reanalysis, which consistently showed > 90% purity. These steps ensured experimental reproducibility and eliminated confounding effects arising from differential handling between GFP⁺ and GFP⁻ cells.

Flow cytometry analysis

Flow cytometry was used exclusively for fluorescence signal quantification and to verify the stability of GFP expression, without physical cell separation. Cells were seeded at 5×10^5 cells per 6 cm dish and treated with 100 ng/mL tetracycline (Sigma-Aldrich) for 19 h prior to analysis for the induced condition or left untreated for the non-induced control. After treatment, cells were detached with trypsin (HyClone), washed with phosphate-buffered saline, and resuspended in 1 mL of PBS. GFP fluorescence was analyzed using a BD FACS Calibur flow cytometer (BD Biosciences) equipped with the FL1 channel detector to capture GFP excitation. In the absence of tetracycline, no measurable GFP fluorescence above the background level was detected in either HeLa or 293 GFP⁺ cultures, indicating that leaky promoter activity, if present, was below the detection threshold. Data were collected using BD CellQuest Pro software and presented as histograms showing the proportion of GFP-positive cells.

Results

Before performing the long-term competition assays, we verified that GFP expression alone did not affect cellular growth or fitness. To this end, we conducted control experiments to confirm that the applied genetic modification was truly fitness-neutral. As shown in Fig. 1 and Table S1 (Supplementary Information), a basic proliferation assay alone was not sensitive enough to detect differences in growth dynamics between GFP⁺ and GFP⁻ cells. Additionally, because the GFP promoter may exhibit leaky activity, we confirmed that activation of the GFP gene under tetracycline induction had no detectable effect on overall fitness or proliferation behavior. To provide a more quantitative assessment, we calculated the specific growth rate (μ, h^{-1}) for each experimental condition from the exponential phase of the growth curves (Fig. S3 and Table S2, Supplementary Information). The μ values were estimated by linear regression of ln(cell number) versus time, using data from at least 3 independent biological replicates. For HeLa cells, the mean μ values were 0.035 ± 0.004 h^{-1} for GFP⁻ and 0.035 ± 0.004 h^{-1} for GFP⁺ cells under non-induced conditions. Continuous tetracycline induction and a 24-hour tetracycline pulse resulted in comparable rates (μ = 0.034 ± 0.004 h^{-1} and 0.035 ± 0.004 h^{-1}, and 0.035 ± 0.004 and 0.034 ± 0.004, respectively). Similarly, for 293 cells, the average μ values were 0.036 ± 0.003 h^{-1} for GFP⁻ and 0.032 ± 0.003 h^{-1} for GFP⁺ cultures, with no substantial differences under any induction regime. Continuous tetracycline induction and a 24-hour tetracycline pulse resulted in comparable rates (μ = 0.036 ± 0.001 h^{-1} and 0.034 ± 0.003 h^{-1}, and 0.036 ± 0.003 and 0.033 ± 0.004, respectively). Statistical comparisons performed using a two-tailed Student's *t*-test confirmed that the observed differences were not statistically significant ($p > 0.05$) across all tested conditions (non-induced, continuous, and pulse tetracycline induction). Data supporting these observations are presented in Table S3 (Supplementary Information. To further assess whether tetracycline treatment influenced growth within each cell line and expression background, we compared the μ values between the three experimental conditions: non-induced, continuous tetracycline induction, and pulse tetracycline induction. For HeLa GFP⁻ cells, the mean μ values across these conditions were 0.035 ± 0.004, 0.034 ± 0.004, and 0.035 ± 0.004 h^{-1}, respectively. For HeLa GFP⁺ cells, the corresponding μ values were 0.035 ± 0.004, 0.035 ± 0.004, and 0.034 ± 0.004 h^{-1}. Similarly, for 293 GFP⁻ cells, μ values were 0.036 ± 0.003, 0.036 ± 0.001, and 0.036 ± 0.003 h^{-1}, while for 293 GFP⁺ cells, they were 0.032 ± 0.003, 0.034 ± 0.003, and 0.033 ± 0.004 h^{-1}, respectively. A one-way ANOVA performed within each group (HeLa GFP⁻, HeLa GFP⁺, 293 GFP⁻, 293 GFP⁺) revealed no statistically significant differences in specific growth rates among the three conditions ($p > 0.05$). Subsequent Tukey's post-hoc tests confirmed the absence of significant pairwise differences between

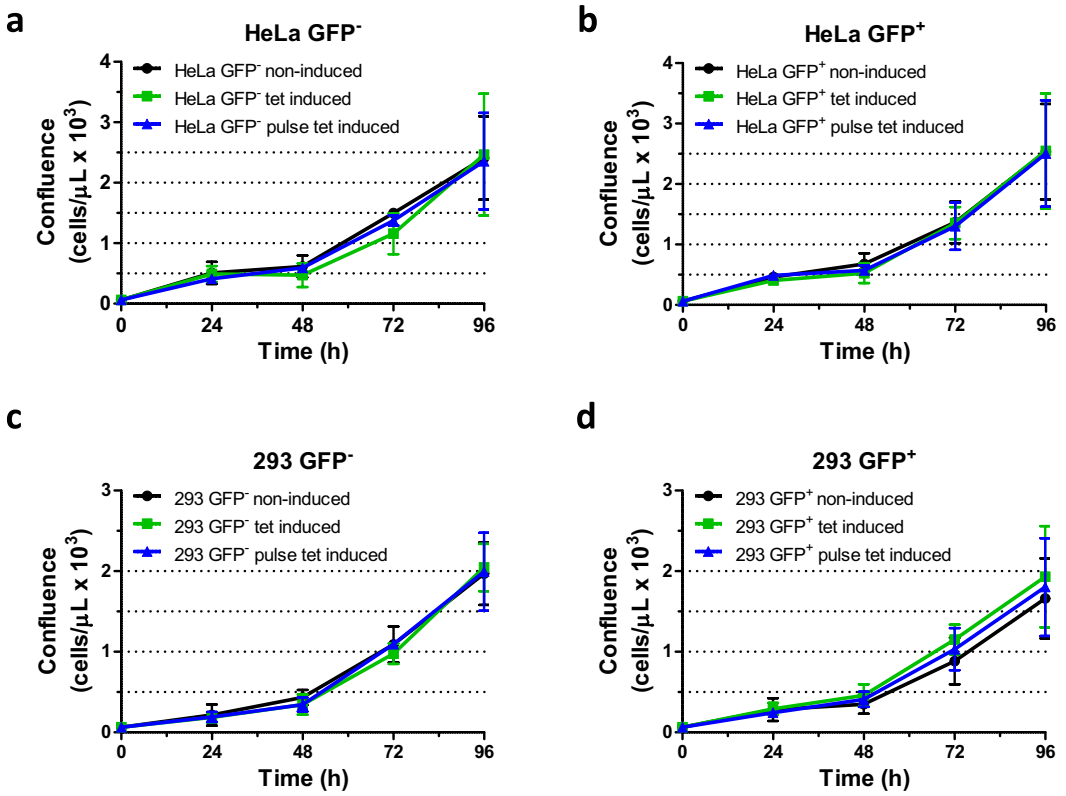

Fig. 1. Proliferation rates of HeLa and 293 cells with and without GFP expression under tetracycline induction. Proliferation was measured in the absence of tetracycline (non-induced), under continuous tetracycline induction (tet induced), or following a 24-hour tetracycline pulse (pulse tet induced, transient induction). (**a**) HeLa GFP$^-$; (**b**) HeLa GFP$^+$; (**c**) 293 GFP$^-$; (**d**) 293 GFP$^+$. Data are presented as mean ± SD from at least three independent biological replicates. Specific growth rates (μ, h^{-1}) were calculated from the exponential phase of the growth curves using linear regression of ln(cell number) *versus* time. Mean μ values were compared between GFP$^-$ and GFP$^+$ cells as well as among the induction conditions, using two-tailed Student's *t*-test or one-way ANOVA followed by Tukey's post-hoc test. No statistically significant differences were observed between GFP$^-$ and GFP$^+$ cells or between induction regimes ($p > 0.05$). Ln of growth curves and statistical analyses are provided in Tables S3 and S4 (Supplementary Information).

non-induced, continuous, and pulse tetracycline treatments in all analyzed groups (Table S4, Supplementary Information). These results indicate that tetracycline exposure and GFP expression do not measurably influence the intrinsic growth kinetics of either HeLa or 293 cells. Thus, both the proliferation data and the quantitative growth-rate analysis support the conclusion that the introduced GFP expression system is fitness-neutral with respect to cellular fitness. This was expected, as a study by Naama Barkai[53] demonstrated that the cost of expressing a single copy of the *GFP* gene is negligible. It is also well established that a proliferation assay is not sensitive enough to detect slight differences in fitness that can be revealed by a competition test[54].

To determine whether subtle differences in cellular fitness could be detected between cells with active and inactive GFP expression, we performed a short-term competition assay (Fig. 2 and Table S5, Supplementary Information). This short-term co-culture experiment was designed both to establish a baseline reference for the subsequent long-term competition assays and to test whether the tetracycline-inducible GFP marker system introduces any detectable fitness bias. Specifically, we tested the hypothesis that activation of the GFP gene imposes a fitness cost. The null hypothesis was that GFP$^+$ and GFP$^-$ cells proliferate at approximately equal rates and that GFP activation does not alter competitive outcomes. If GFP expression imposed a fitness cost, GFP$^-$ cells would be expected to outcompete GFP$^+$ cells specifically under induced conditions, while both populations would proliferate at similar rates in the absence of induction. Conversely, if competitive differences were caused by pre-existing clonal variation, background mutations, or other marker-independent factors, GFP induction would not be expected to systematically alter the outcome of the competition. Because the subsequent long-term competition experiments (Fig. 3) were conducted under non-induced conditions, it was also important to determine whether the GFP construct itself, independent of induction, or possible basal promoter leakiness could influence competitive dynamics. GFP$^+$ and GFP$^-$ cells were mixed at an approximate 1:1 ratio, and competition outcomes under GFP induction were compared with those under non-induced conditions. In HeLa cells, the GFP$^+$ fraction decreased slightly faster upon GFP induction; however, this difference did not reach statistical significance ($p > 0.05$, Fig. 2a). It is worth noting that in this initial competition experiment, the fraction of HeLa GFP$^+$ cells cultured without tetracycline remained practically unchanged, suggesting fitness-

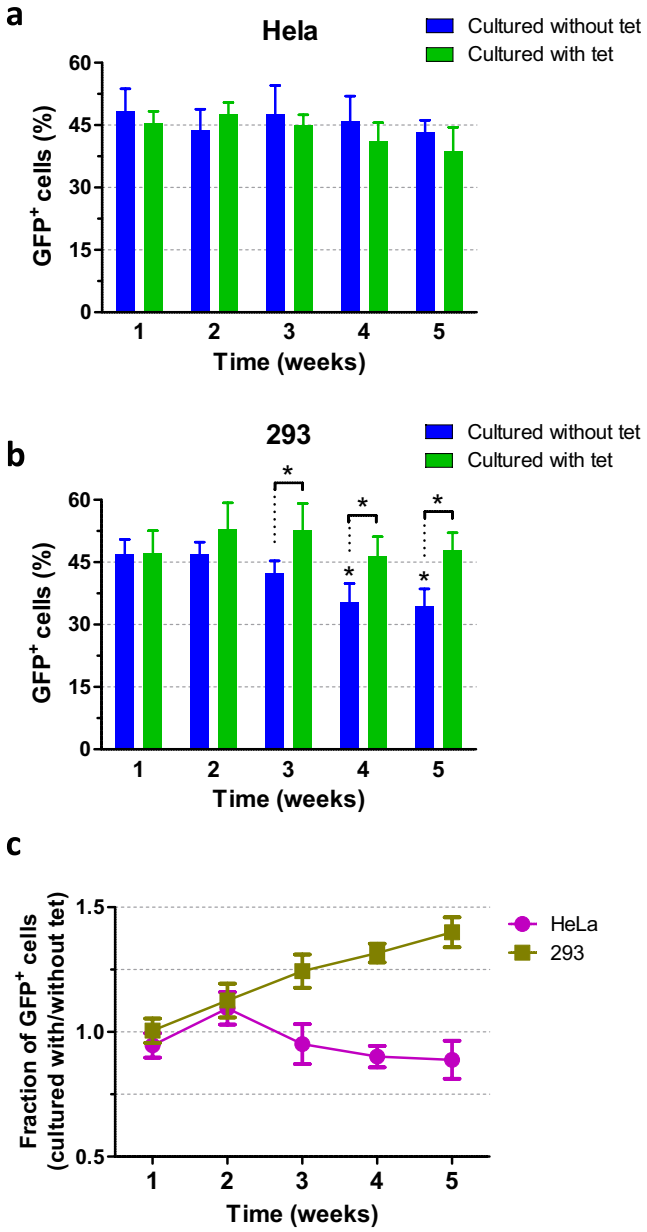

Fig. 2. Short-term competition assay between GFP⁺ (induced or non-induced) and GFP⁻ cells testing the fitness-neutrality of GFP expression and tetracycline induction**.** (**a**) HeLa and (**b**) 293 GFP⁺ cells were mixed with their corresponding GFP⁻ cells at an approximate 1:1 ratio at the beginning of the experiment to test whether GFP expression affected the cell fitness. GFP expression was controlled using a tetracycline-inducible promoter (Tet-On system) and induced with 1 µg/mL tetracycline (**c**). The proportion of GFP⁺ cells in mixed GFP⁺/GFP⁻ co-cultures was monitored over time under induced and non-induced conditions for both cell lines. GFP fluorescence was detected by flow cytometry using a BD FACS Calibur system. Data represent the mean ± SD from three independent biological replicates, each initiated from separate cell cultures. Statistical analyses were performed using a two-tailed Student's *t*-test (for GFP⁺ *vs* GFP⁻) and one-way ANOVA followed by Tukey's post hoc test for comparisons among induction regimes (* $p < 0.05$).

neutral behavior under non-induced conditions. In 293 cells, the GFP⁺ fraction increased slightly upon GFP activation (Fig. 2b), indicating that GFP induction does not impose a detectable fitness cost. Notably, only the non-induced 293 cells showed a small but statistically significant reduction in the growth rate of GFP⁺ cells ($p < 0.05$, Fig. 2b). Because this effect was not observed under induction, it is unlikely to result from GFP expression itself or from toxicity caused by integration of the GFP construct into the genome. This interpretation is further supported by the long-term competition experiments under non-induced conditions (Fig. 3), in which 293 GFP⁺ cells did not show a persistent competitive disadvantage and instead gradually increased in frequency during the later phase of the experiment. Therefore, the small short-term difference observed here is more likely to reflect

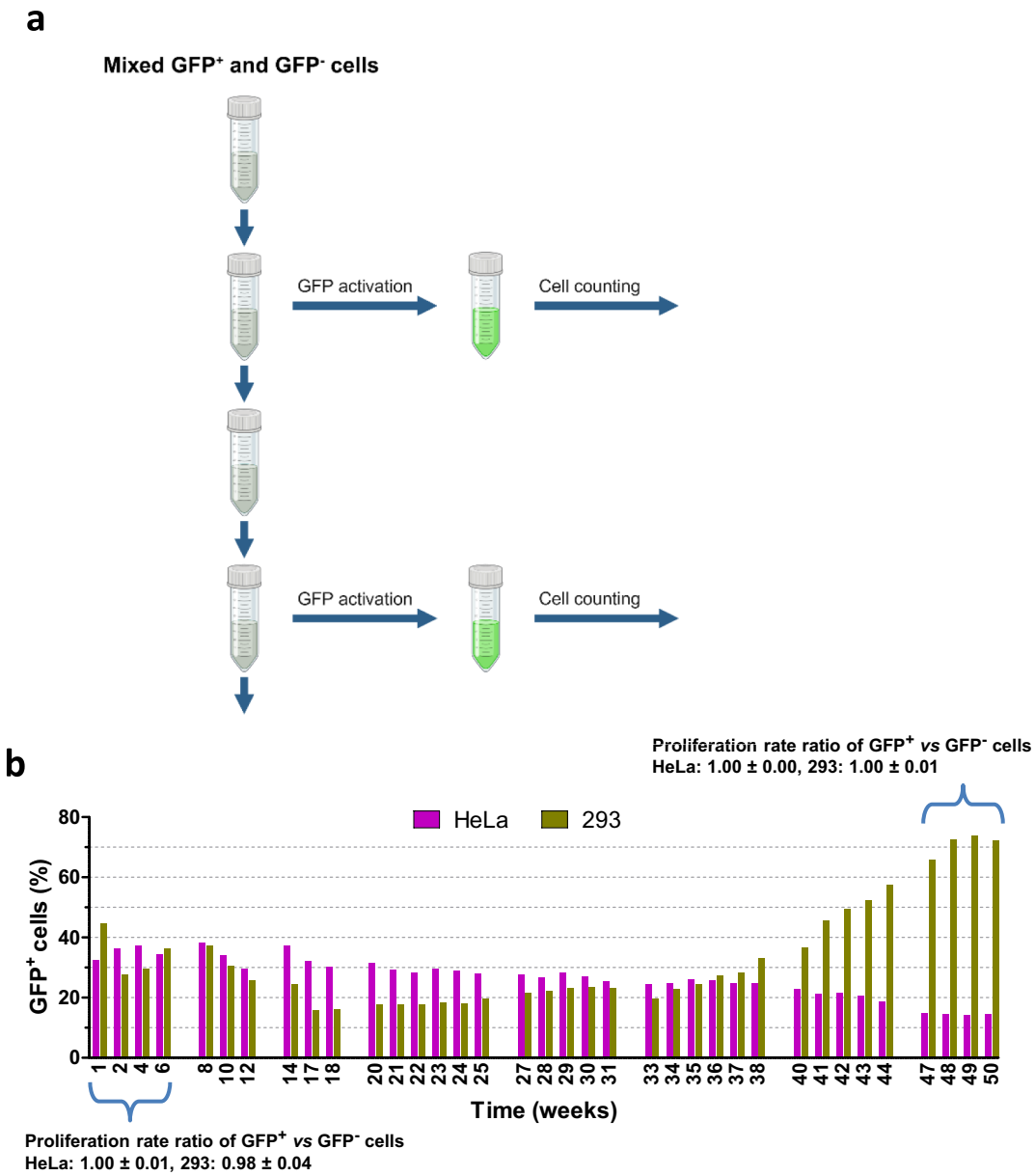

Fig. 3. Long-term co-culture experiment tracking population dynamics of GFP⁺ and GFP⁻ cells. A long-term competition assay was performed over 12 months to monitor evolutionary changes between GFP⁺ and GFP⁻ populations in HeLa and 293 cells. Cells were co-cultured in the absence of tetracycline to ensure that GFP remained uninduced and functioned solely as a marker with no detectable fitness effect. (**a**) Schematic representation of the experimental design. GFP⁺ and GFP⁻ subpopulations were mixed at an initial 1:1 ratio and propagated through serial passages under constant conditions. Created with BioRender.com. (**b**) Quantitative results showing changes in the proportion of GFP⁺ cells over approximately 50 weeks (~350 generations). GFP fluorescence was detected by flow cytometry using a BD FACS Calibur.

subtle ancestral clonal variation, background mutations, stochastic drift, or experimental variability rather than a stable GFP-associated fitness cost.

Having confirmed that GFP expression and tetracycline treatment did not measurably influence cell proliferation or fitness dynamics, we next performed long-term competition assays to examine whether spontaneous adaptive or more adapted phenotypes could emerge during extended co-culture of GFP⁺ and GFP⁻ populations (Fig. 3 and Table 6, Supplementary Information). In this experiment, co-evolving populations of HeLa and 293 cells, initially differing only by the presence or absence of an inducible, fitness-neutral marker gene (GFP) integrated into the genome, were mixed. Throughout the experiment, the *GFP* gene was not induced; the marker served solely to distinguish GFP-positive and GFP-negative cells. At the beginning of the experiment, we observed hallmarks of neutral evolution. During the first weeks, the frequencies of GFP-positive cells fluctuated. Later, the proportion of GFP⁺ HeLa cells steadily declined, reaching approximately 15% of the total cell population at the end of the experiment. In contrast, the proportion of GFP⁺ 293 cells initially decreased

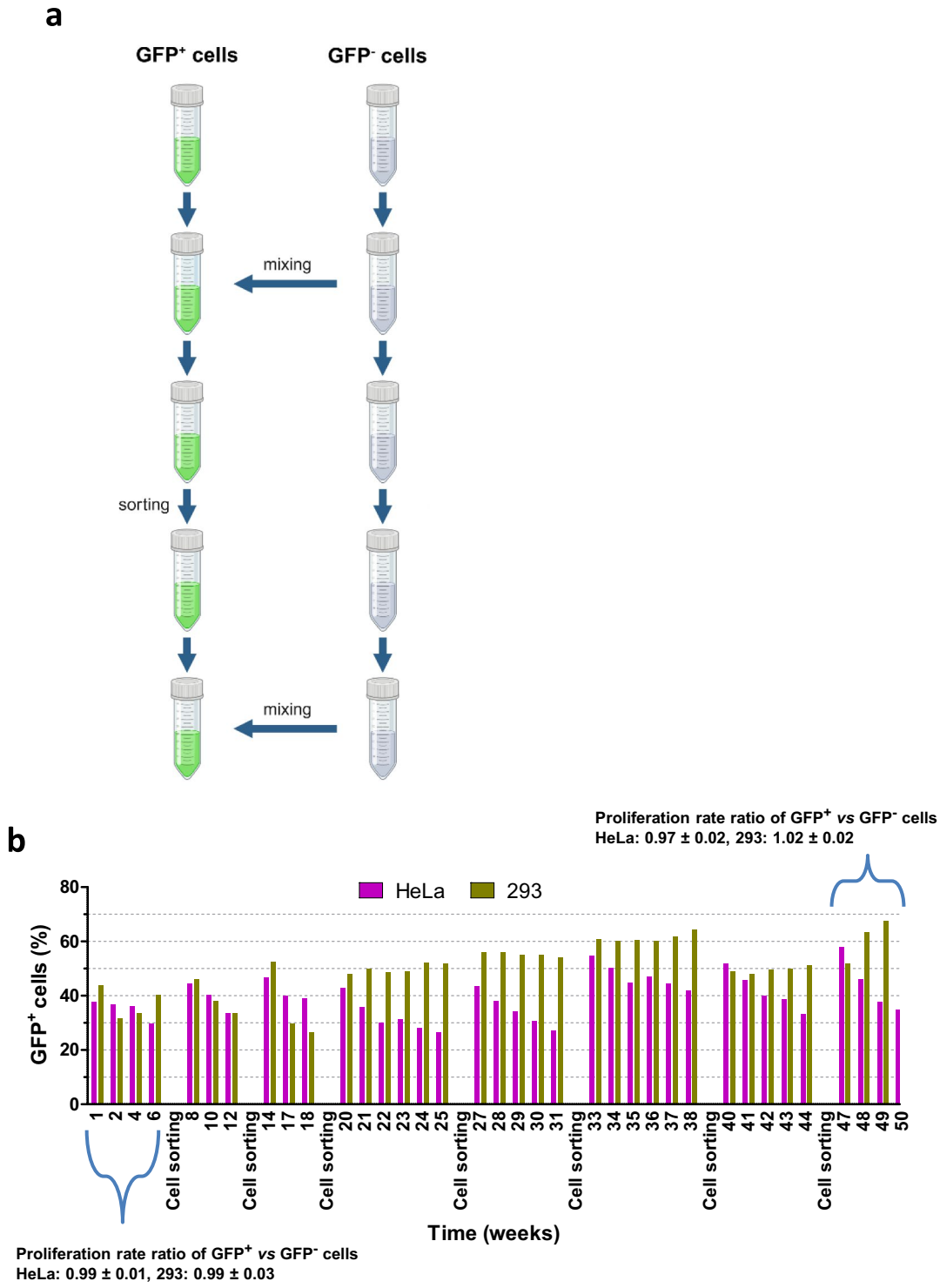

to about 16% during the first four months but subsequently began to increase. After 12 months, GFP⁺ cells constituted roughly 72% of the 293 population. However, this shift occurred slowly over many passages and did not resemble a rapid clonal sweep. Based on the calculations presented below and in Fig. 3, the inferred fitness advantage was extremely small ($s \approx 0.005$), consistent with weak selection acting over long time scales and modulated by genetic drift.

Throughout the experiment, we did not observe rapid expansion of more-adapted clones that led to the extinction of competing populations or to the complete dominance of either GFP⁺ or GFP⁻ cells. For this analysis, we assumed that a more adapted, competitively dominant clone would possess a fitness advantage greater than 0.2. According to Wahl's formula, as described in the Methods section, the probability that such a mutation would lead to the emergence of more adapted clones exceeds 0.2. This formula applies to populations with fluctuating sizes. The rapid expansion by such a more adapted clone would be expected to occur within approximately 100 generations, at which point its population would overtake the entire population. This expectation is based on the following calculation: after 100 generations, a clone carrying a beneficial mutation with a fitness advantage

◀**Fig. 4**. Velicer-type competition assay between "evolving" GFP⁺ and "non-evolving" GFP⁻ cells. (**a**) Schematic representation of the experimental design. The assay was modeled after Velicer's bacterial social evolution framework to test whether GFP⁺ cells could evolve competitively advantageous or antagonistic traits under repeated encounters with non-evolving GFP⁻ cells. In each cycle, GFP⁺ cells were co-cultured for four weeks (~28 generations) with independently propagated GFP⁻ cells. After each cycle, GFP⁺ cells were isolated using a BD FACSAria III cell sorter and transferred to a new flask containing freshly prepared GFP⁻ cells to begin the next cycle. This design ensured that GFP⁻ populations remained non-evolving while GFP⁺ cells could potentially accumulate adaptive mutations. In this Velicer-type assay, each cycle consisted of four weeks of co-culture followed by sorting-based enrichment of GFP⁺ cells and reintroduction into a freshly prepared GFP⁻ population. Therefore, the transient increase in GFP⁺ frequency immediately after each sorting step reflects enrichment/reset of starting proportions rather than a true adaptive fitness increase of GFP⁺ cells. Created with BioRender.com. (**b**) Quantitative results showing changes in the frequency of GFP⁺ cells over 12 successive cycles (12 months total). GFP fluorescence was detected by flow cytometry using a BD FACS Calibur. In HeLa cultures, the GFP⁻ fraction gradually increased during most cycles, indicating a consistent selective advantage. The transient increase in the GFP⁺ fraction immediately after sorting reflects the enrichment of GFP⁺ cells by the FACS step before mixing with GFP⁻ cells. In contrast, 293 cells displayed an initial decrease in GFP⁺ frequency followed by long-term stabilization. The transient increases in GFP⁺ frequency after sorting reflect enrichment during the FACS step. The estimated growth-rate differences between competing populations were small ($\Delta\mu < 0.04$ per generation) and remained similar throughout the experiment. These dynamics are consistent with weak selection, leading to gradual and limited changes in population structure without rapid clonal sweeps or fixation, and do not support the emergence of strongly competitive or antagonistic phenotypes under constant laboratory conditions.

of 0.2 would be more than 1.2^{100} (≈83 million) times more abundant than any competing clone. Given that our experimental population consisted of approximately 10^5 individuals, such an advantage would be sufficient for the competitively dominant mutant to dominate the population within one hundred generations. Since our experiment spanned roughly 350 generations, we conclude that no rapid expansions by a more adapted clone occurred during the first 250 generations.

The results also indicated that the differences in fitness between competing clones were very small. Using our data, we estimated the growth rate advantage of the outcompeting clones. After 50 weeks (approximately 350 generations), in both cases, the outcompeting clone constituted less than 85% of the total cell population. Assuming continuous exponential growth, population size can be described by the equation e^{mt}, where m is the growth rate, and t is time (in generations). We used this formula to estimate the difference in growth rates between the outcompeting and losing clones per generation, expressed as $m_o - m_l$. As mentioned above, the experiment spanned approximately 350 generations (t = 350). After this period, the ratio of outcompeting to losing populations in HeLa cells was less than 0.85/0.15.

Therefore, $e^{350mo}/e^{350ml} < 0.85/0.15$ and $350*(m_o - m_l) < \ln(0.85/0.15)$.

Resolving this inequality led to $m_o - m_l < 0.00495$.

Direct measurements of growth rates, performed weekly during the first and last months of the experiment (Fig. 3b), confirmed the previously estimated values. These results further demonstrate that differences in growth rates between competing clones were extremely small and became detectable only after multiple generations. The observed fluctuations in subpopulation sizes could result from either genetic drift or a minor selective advantage. To distinguish between these possibilities, we simulated fitness-neutral evolution 1,000 times. Under fitness-neutral conditions, the probability that an outcompeting population would exceed 65% was $p < 0.001$, indicating that the observed fluctuations were largely consistent with a small selective advantage. This analysis indicates that sporadic beneficial mutations arose in the evolving cell lines, leading to the gradual expansion of either GFP⁺ or GFP⁻ cells.

We next examined whether there were indications of an evolutionary arms race between competing cells. In such a scenario, clones continuously evolve traits that confer a fitness advantage, while competitors simultaneously evolve counter-adaptations. Cells unable to mount such evolutionary responses would be outcompeted. To test this, we evolved GFP⁺ cells in competition with GFP⁻ cells that were prevented from evolving. This approach was inspired by the classical observation that HeLa cells are sensitive to apoptosis induced by tumor necrosis factor (TNF)-related apoptosis-inducing ligand[55]. We therefore hypothesized that cells could evolve mechanisms conferring a strong selective advantage over non-evolving competitors. For example, such variants might release growth-inhibiting factors (*e.g.*, inducing apoptosis) while simultaneously losing receptors for these factors. In this experiment, GFP⁺ cells were repeatedly co-cultured with independently propagated GFP⁻ populations that could not evolve in parallel, following a Velicer-type competition design (Fig. 4 and Table 7, Supplementary Information). GFP⁺ and GFP⁻ cells were analyzed by fluorescence-activated cell sorting (FACS) at regular intervals during long-term co-culture. The sorting procedure was designed to quantify the proportions of GFP⁺ and GFP⁻ subpopulations and to assess the stability of GFP expression following continuous or transient tetracycline induction. In HeLa cultures, the proportion of GFP⁻ cells gradually increased across co-culture cycles over the 12-month experiment, suggesting a modest yet consistent selective advantage of GFP⁻ cells. In contrast, 293 cultures showed an initial increase in GFP⁻ frequency during the first three cycles, followed by stable population ratios in the subsequent nine months of co-culture with GFP⁺ cells (Fig. 4). Prior to the first sorting, we observed fluctuations consistent with random drift. During the subsequent two cycles, before the second and third sorting steps, GFP⁻ cells gained an advantage in both cell types. This pattern persisted in HeLa cells but was reversed in the GFP⁺ 293 population. Therefore, these results provide no evidence for the evolution

of strongly advantageous clones capable of successfully outcompeting non-evolving competitors that are unable to mount evolutionary responses. In HeLa cells, competition tended to favor the non-evolving population, whereas in 293 cells, competition tended to favor the evolving cells. Estimated differences in growth rates between outcompeting and losing clones were small. In each cycle (~28 generations), the ratio of outcompeting to losing populations remained below 0.75:0.25, corresponding to an estimated growth-rate difference of $m_o - m_l < 0.04$ per generation.

We also examined GFP expression and found it stable throughout the experiment, as assessed by cell sorting. After the one-year-long experiment, GFP^+ and GFP^- cells were correctly sorted. Fig. 5 illustrates the distribution of GFP-expressing and non-expressing cells for the HeLa and 293 cell lines, obtained before the first sorting and after the final sorting. Additionally, by sorting GFP^+ cells weekly, we confirmed that the marker gene was retained throughout the experiment (Fig. 5c and Table 8, Supplementary Information). Therefore, we ruled out the possibility that the observed differences in cell populations resulted from instability of the marker gene's integration.

Discussion

We repeated Roy Kishony's experimental design using human cell lines and did not observe rapid clonal expansions (selective sweeps) of either GFP^+ or GFP^- subclones. In contrast, such rapid clonal takeovers were frequently observed in the original Kishony experiment, which examined competition between *E. coli* populations during the first 300 generations and reported an estimated selection coefficient of $s = 0.054$[47]. Classical long-term evolution experiments in bacteria, most notably Richard Lenski's *E. coli* experiment, have revealed similar evolutionary dynamics during the first several hundred generations[36]. Notably, significant fitness differences of approximately 3% were still detected between 40,000 and 50,000 generations[56]. In contrast, our results suggest that long-term cultured human cell lines evolve substantially more slowly, exhibiting only weak fitness differences and no evidence of rapid clonal sweeps over approximately 300–350 generations. The selective effects inferred in our human cell system were at least an order of magnitude smaller ($s \lesssim 0.005$). These observations suggest that both cancer-derived (HeLa) and immortalized non-cancerous (293) human cell lines are almost perfectly adapted to their standard culture environment. Minor spontaneous mutations arising during routine propagation did not appear to significantly improve cell fitness, and we did not observe rapid clonal takeovers (selective sweeps) of either evolved GFP^+ or GFP^- subclones (Figs. 3 and 4). In this study, "fitness" is defined operationally as a competitive growth advantage under standard *in vitro* culture conditions, quantified by changes in GFP^+/GFP^- frequencies and/or differences in proliferation rate. Importantly, this *in vitro* fitness should not be interpreted as clinical "aggressiveness" and is not directly related to invasion or metastasis. Although the GFP^+ subpopulation increased in frequency in 293 during the later phase of the experiment (Fig. 3), this change was gradual and accumulated over many months rather than reflecting a rapid clonal expansion. Quantitative estimates indicate that the associated selective advantage was very small ($s \approx 0.005$), suggesting a regime of weak selection in which frequency changes proceed. Thus, the observed dynamics are more consistent with minor fitness differences than with the emergence of a strongly beneficial mutant driving rapid clonal expansion.

Before initiating long-term evolution experiments, it was essential to verify that the genetic marker used to distinguish cell populations, the tetracycline-inducible GFP construct, was indeed fitness-neutral with respect to cellular growth and fitness. The short-term experiment presented in Fig. 1 and Fig. S3 demonstrated that continuous, transient, or absent GFP induction did not produce statistically significant differences in proliferation rates or population dynamics in either HeLa or 293 cells. The short-term competition assay (Fig. 2) showed that GFP expression had no measurable effect on proliferation rate or competitive dynamics in either HeLa or 293 cells. This control was critical to exclude the possibility that GFP expression or tetracycline exposure could bias the results of long-term co-culture experiments. Having established this fitness-neutrality, we could interpret the subsequent changes in GFP^+ and GFP^- population ratios (Figs. 3–5) as genuine outcomes of spontaneous evolutionary dynamics rather than artifacts of gene expression or induction. Thus, Fig. 1, Fig. S3, and Fig. 2 provide the methodological foundation for the entire experimental design, ensuring that subsequent results reflect authentic evolutionary processes in the tested cell populations. These findings also highlight the importance of validating marker fitness-neutrality in experimental evolution studies involving mammalian cells. Even subtle metabolic costs of reporter gene expression could, in principle, confound long-term competition outcomes.

We further tested whether beneficial mutations could be selected in cells that outcompete populations unable to mount an evolutionary response, using the methodology adapted from Velicer and colleagues' work on *Myxococcus xanthus*[21]. In this design, GFP^+ cells were repeatedly mixed with independently propagated, "non-evolving" GFP^- cells, enabling GFP^+ cells to potentially evolve exploitative strategies while preventing GFP^- cells from evolving counter-adaptations. It turns out that in HeLa cells, competition tended to favor GFP^- cells that were unable to evolve an evolutionary response (Fig. 4). This observation suggests that an evolutionary arms race between cells may not occur. Alternatively, evolution may be too slow to be detected over the course of one year. Importantly, although measurable differences in growth rates were detected ($\Delta\mu < 0.04$ per generation), these correspond to weak selection that is insufficient to drive rapid clonal sweeps or fixation. In this context, we define evolutionary stability as the absence of strong directional selection that leads to the dominance of a single clone, rather than the complete absence of fitness differences.

On closer inspection, we observed indications of neutral evolution before the first sorting. Subsequently, non-evolving GFP^- cells gained an advantage in both 293 and HeLa populations. This pattern was consistent across the Velicer-type experiments, in which GFP^+ and GFP^- cells were repeatedly mixed, consistently showing a modest but reproducible advantage of the GFP^- subpopulation. Because the GFP marker remained inactive and was experimentally validated as fitness-neutral, this early advantage is unlikely to reflect marker effects or

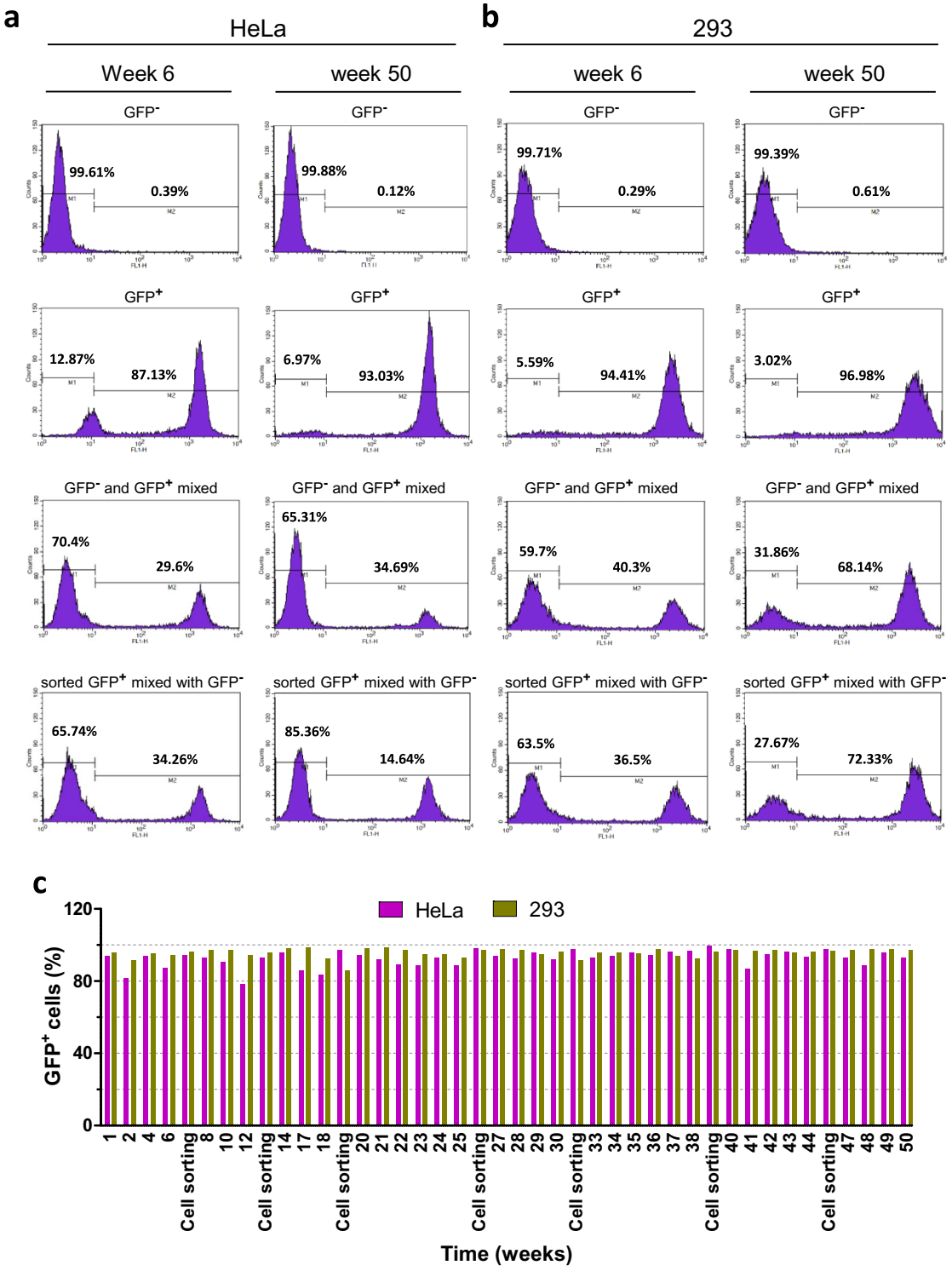

Fig. 5. Flow cytometry analysis confirming the stability of GFP expression in HeLa and 293 cell lines during the long-term co-culture experiment. Flow cytometry was used to verify GFP expression stability and marker gene integrity after one year of continuous culture and repeated sorting. (**a**) and (**b**) Representative flow cytometry histograms showing the distribution of GFP fluorescence intensity in HeLa and 293 cell populations, respectively, before the first sorting (initial population) and after the final sorting (post-12-month co-culture). Distinct peaks corresponding to GFP⁺ and GFP⁻ subpopulations confirm that the inducible GFP construct remained stably integrated and expressed upon induction. (**c**) Weekly sorting of GFP⁺ cells confirmed that the marker gene was retained throughout the experiment, with no detectable loss of fluorescence signal or decline in the GFP⁺ fraction. Data were obtained using a BD FACS Calibur system for fluorescence detection and a BD FACSAria III cell sorter for subpopulation isolation.

random drift alone. Instead, the initial advantage of GFP⁻ cells may instead reflect the accumulation of mildly deleterious mutations in GFP⁺ cells during successive passages or subtle differences in clonal physiology unrelated to GFP expression. Indeed, a recent study demonstrated that HeLa populations carry substantial genetic load and chromosomal instability, which can influence fitness variation among subclones[46]. Interestingly, after approximately 4 months, 293 GFP⁺ cells acquired a slight selective advantage, potentially reflecting compensatory changes that mitigate the initial cost of the transgene or weak adaptive evolution. In contrast, the advantage of GFP⁻ cells in HeLa populations remained stable throughout the experiment (Figs. 3 and 4). Flow cytometric measurements confirmed that GFP expression was tightly regulated by the tetracycline-inducible promoter. In the absence of tetracycline, GFP⁺ cells exhibited fluorescence indistinguishable from that of GFP⁻ controls, confirming that leaky expression was below detection limits. Upon induction, GFP fluorescence increased sharply, with well-separated GFP⁺ and GFP⁻ populations (Fig. 5). Overall, although somatic evolution occurred, fitness differences between competing subclones remained small and did not lead to sustained expansions.

Importantly, interpretation of long-term shifts in GFP⁺/GFP⁻ frequencies requires consideration of potential ancestral fitness differences between the starting subclones. Although the GFP marker system was designed to be fitness-neutral and control assays did not reveal consistent large effects of GFP induction (Figs. 1–2), our results indicate that the ancestral GFP⁺ and GFP⁻ lineages were not necessarily identical in fitness. Such baseline differences may arise from minor physiological variation, genetic load, or background mutations accumulated during cell line establishment and can generate gradual frequency shifts over serial passaging even in the absence of strong adaptive sweeps. Therefore, long-term trajectories should be interpreted primarily as deviations from the ancestral baseline rather than as absolute effects of GFP integration or expression. In this framework, the key observation is not the presence of small early shifts per se, but the absence of rapid clonal expansions and the persistence of only weak selection coefficients (*e.g.*, $s \lesssim 0.005$ in HeLa). In 293 cells, the gradual increase in GFP⁺ frequency during the later phase of the experiment is thus more consistent with weak compensatory changes and/or drift under near-neutral dynamics than with a direct beneficial effect of GFP expression.

We did not perform whole-*genome* sequencing, as our primary goal of this study was to evaluate evolutionary stability at the phenotypic and population levels rather than to identify the specific genetic basis of adaptation. Because the observed fitness differences were extremely small and no dominant mutant subclones emerged, sequencing at this stage would likely yield an overwhelming background of fitness-neutral mutations, making it difficult to distinguish adaptive variants without additional experimental approaches. Moreover, adaptive changes may also arise through epigenetic mechanisms, such as chromatin remodeling or DNA methylation, which cannot be detected by standard genome sequencing. Identifying true adaptive mutations in this context would therefore require complementary analyses, including population sequencing, lineage tracking, or parallel evolution experiments. Importantly, no variants with increased competitive effects on other cells were detected, further supporting the conclusion that both cell lines exhibit stable, evolutionarily balanced coexistence under constant laboratory conditions.

A key limitation of the present study is that the long-term evolution experiment was performed exclusively under standard *in vitro* conditions. Therefore, the observed evolutionary dynamics cannot be directly extrapolated to clinically relevant contexts such as drug treatment, immune interactions, or the complex and heterogeneous tumor microenvironment. Instead, our results should be interpreted as a baseline evolutionary reference describing how long-term cultured cancer cell lines behave in the absence of strong external selective pressures. In this framework, our findings suggest that HeLa (and similarly, 293) cells may be close to a near-optimal adaptive state under standard laboratory culture conditions, with limited evolutionary plasticity in constant-growth environments. Importantly, this conclusion is relevant for experimental reproducibility in preclinical research and provides a useful point of comparison for studies that impose strong selection. As previously noted, earlier studies have shown that artificial selection imposed by drug treatment can reactivate adaptive evolution in otherwise slowly evolving cell populations [31–33]. Future work should examine whether clinically relevant selective pressures similarly reinstate adaptive evolution, for example, through long-term evolution experiments involving drug exposure, hypoxia, nutrient limitation, or other microenvironmental constraints. Such experiments would help determine the extent to which the evolutionary potential of long-term cultured cell lines depends on heterogeneous and clinically relevant selection regimes. Consistent with this interpretation, the lack of clear expansion by faster-growing or better-adapted subpopulations in our long-term competition assays suggests that both the HeLa and 293 cell lines may already be close to their adaptive optima under standard *in vitro* conditions. However, we acknowledge that this conclusion serves as a working hypothesis and warrants further experimental validation. Several alternative explanations could account for the observed evolutionary stability. First, micro-adaptive evolution may be constrained by the limited ecological complexity of standard culture environments, which provide constant nutrient availability and uniform selective pressures. In such settings, potential fitness improvements may be marginal and difficult to detect within realistic experimental timescales. Second, epigenetic buffering mechanisms, such as chromatin remodeling, DNA methylation, and post-transcriptional regulation, may stabilize gene expression and phenotype, thereby reducing the impact of weakly beneficial mutations. This form of canalization could limit observable phenotypic divergence even if genetic variability continues to accumulate. Third, cell evolution under laboratory conditions may be extremely slow, as the cells have likely already reached an almost optimal state. This mechanism is consistent with theoretical models of evolution in stable environments, where adaptation proceeds slowly, and mutation-driven diversity does not necessarily translate into fitness improvement. To discriminate among these possibilities, future studies will experimentally alter environmental conditions to introduce stronger and more heterogeneous selective pressures. Planned experiments include long-term culture under reduced serum concentration, hypoxia, moderate temperature shifts, and exposure to cytotoxic or metabolic stressors, conditions expected to activate adaptive responses. Comparing evolutionary trajectories in such perturbed

environments with those observed in the present study will help determine whether the apparent stability of HeLa and 293 cells reflects true evolutionary constraints or merely the absence of environmental challenges.

From a broader evolutionary perspective, our findings are consistent with the view that adaptation and competition of cells in multicellular systems are shaped by ecological structure and resource distribution. The recently formulated theory of the evolutionary ecology of organs extends this view to the tumor microenvironment, proposing that cancer cells evolve local adaptations to distinct organ niches to ensure their survival and proliferation [57,58]. Rapid selection of more adapted subclones has been observed during the early stages of tumor evolution, often within the first 10–20 population doublings (before the tissue reaches ~32,000 cells), where fitness advantages can reach 20–80%[59]. Such subclones display distinct local adaptations in different organs that can be interpreted as strategies against specific host cell types[23]. Recent theoretical predictions suggest that after 30–90 days, a significant fraction of the population belongs to clones that carry beneficial mutations. However, the scale of rapid clonal expansions by beneficial mutants is less predictable in rapidly growing cell populations[60]. In contrast, our results suggest that under constant laboratory conditions, cancer cell evolution primarily generates clones optimally adapted to their immediate ecological niche rather than adaptations involving increased competitive or antagonistic interactions. Interestingly, it has been shown that breast cancer cells can induce apoptosis in HeLa cells through intercellular signaling mechanisms[55], supporting the concept that interactions between genetically distinct cancer cell populations may influence cell survival and competition outcomes. Therefore, future studies on the evolution of competition between different genetically distinct cell lines may lead to the discovery of novel tumor-suppressing factors. From a clinical perspective, our evolutionary experiments can be considered a model for the evolution of solid tumors, as spatial structure has been shown to influence cancer cell evolution[61]. The evolutionary dynamics of laboratory cell lines resemble those of solid tumors, where genetically similar cancer cells compete for limited space and nutrients. Ultimately, our study indicates that HeLa and 293 cells are well adapted to standard *in vitro* conditions, suggesting that spontaneous evolutionary divergence into behaviorally distinct subpopulations is unlikely under stable environments. This observation is important because cancer cell lines are widely used to study the evolution of drug resistance, in which strong selective pressures drive rapid adaptive change, and as *in vivo* models of tumor invasion in immunocompromised mice, in which additional microenvironmental adaptation is expected. Taken together, our findings demonstrate that long-term cultured human cell lines, including those derived from cancer, exhibit exceptionally slow evolutionary dynamics under standard laboratory conditions. The absence of detectable fitness divergence or the emergence of dominant adaptive clones suggests that these populations have reached a near-optimal equilibrium with their environment. Spontaneous mutations that arise during culture appear to have minimal impact on overall fitness, reflecting the high degree of evolutionary saturation in these systems.

Conclusions

Our results demonstrate that human cell cultures, including those derived from cancer cells, evolve very slowly under standard laboratory conditions. Spontaneous mutations in these cells have minimal impact on fitness, suggesting that both cancerous and non-cancerous cell lines are already close to an optimal adaptation to their culture environment. In contrast to cancer cells in *vivo*, which can employ complex mechanisms to influence surrounding cells and gain competitive advantages, no more adapted or competitively dominant clones emerged in our long-term *in vitro* experiments. Even under conditions designed to favor the selection of adaptive or competitively dominant phenotypes, GFP^+ cells did not develop mechanisms enabling them to outcompete GFP^- cells. These observations highlight a fundamental distinction between cellular evolution *in vivo* and *in vitro*. While *in vivo* evolution generates highly competitive, rapidly adapting subclones in response to heterogeneous and dynamic selective pressures, evolution in laboratory cell cultures appears constrained by environmental stability and limited ecological complexity. Consequently, long-term cultured human cell lines, even those originating from cancers, have intrinsic limitations as models for studying somatic evolution, cellular cooperation, and the emergence of more adapted or parasitic behaviors. Nevertheless, their evolutionary stability makes them valuable systems for controlled investigations of mutation accumulation, genetic drift, and adaptive limits under constant environmental conditions. However, several alternative hypotheses may explain the observed evolutionary stasis, including ecological constraint, epigenetic buffering, and selection–drift equilibrium. We propose that introducing environmental heterogeneity, such as nutrient limitation, hypoxia, or pharmacological stress, could reactivate adaptive dynamics and reveal latent evolutionary potential within these otherwise stable cell lines. Future experiments along these lines will directly test whether the lack of detectable evolution in our study reflects true evolutionary saturation or is merely attributable to the stabilizing effects of standard culture conditions.

From a broader biomedical perspective, these results underscore that long-term cultured human cell lines, though invaluable for controlled studies of genetic drift and mutation accumulation, have intrinsic limitations as clinical models of tumor evolution and adaptation. Their evolutionary stability, however, makes them ideal systems for dissecting the boundaries between fitness-neutrality and selection, providing a quantitative framework for understanding how environmental complexity shapes the pace and direction of somatic evolution.

Data availability

All data generated or analyzed during this study are included in this published article and its Supplementary Information file.

Received: 23 October 2025; Accepted: 11 June 2026
Published online: 19 June 2026

References

1. Boveri, T. Concerning the origin of malignant tumours by theodor boveri. translated and annotated by henry harris. *J. Cell Sci.* **121**, 1–84 (2008).
2. Nowell, P. C. The clonal evolution of tumor cell populations. *Science* **194**, 23–28 (1976).
3. Yates, L. R. & Campbell, P. J. Evolution of the cancer genome. *Nat. Rev. Genet.* **13**, 795–806 (2012).
4. Podlaha, O., Riester, M., De, S. & Michor, F. Evolution of the cancer genome. *Trends Genet.* **28**, 155–163 (2012).
5. Boland, C. R. & Goel, A. Somatic evolution of cancer cells. *Sem. Cancer Biol.* **15**, 436–450 (2005).
6. Lambert, G. et al. An analogy between the evolution of drug resistance in bacterial communities and malignant tissues. *Nat. Rev. Cancer* **11**, 375–382 (2011).
7. Wu, A. et al. Ancient hot and cold genes and chemotherapy resistance emergence. *Proc. Natl. Acad. Sci.* **112**, 10467–10472 (2015).
8. Easwaran, H., Tsai, H.-C. & Baylin, S. B. Cancer epigenetics: tumor heterogeneity, plasticity of stem-like states, and drug resistance. *Mol. Cell* **54**, 716–727 (2014).
9. Marusyk, A., Almendro, V. & Polyak, K. Intra-tumour heterogeneity: a looking glass for cancer?. *Nat. Rev. Cancer* **12**, 323–334 (2012).
10. Chang, M. T. et al. Identifying recurrent mutations in cancer reveals widespread lineage diversity and mutational specificity. *Nat. Biotechnol.* **34**, 155–163 (2016).
11. Gerl, R. & Vaux, D. L. Apoptosis in the development and treatment of cancer. *Carcinogenesis* **26**, 263–270 (2005).
12. Evan, G. I. & Vousden, K. H. Proliferation, cell cycle and apoptosis in cancer. *Nature* **411**, 342–348 (2001).
13. Williams, G. H. & Stoeber, K. The cell cycle and cancer. *J. Pathol.* **226**, 352–364 (2012).
14. Thompson, S. L., Bakhoum, S. F. & Compton, D. A. Mechanisms of Chromosomal Instability. *Curr. Biol.* **20**, R285–R295 (2010).
15. Watanabe, N., Okochi, E., Mochizuki, M., Sugimura, T. & Ushijima, T. The presence of single nucleotide instability in human breast cancer cell lines. *Cancer Res.* **61**, 7739–7742 (2001).
16. Ben-David, U. & Amon, A. Context is everything: aneuploidy in cancer. *Nat. Rev. Genet.* **21**, 44–62 (2020).
17. Warburg, O. On the origin of cancer cells. *Science* **123**, 309–314 (1956).
18. Geiger, T. R. & Peeper, D. S. Metastasis mechanisms. *Biochimica et Biophysica Acta (BBA) – Rev. Cancer* **1796**, 293–308 (2009).
19. Alison, M. R., Lin, W.-R., Lim, S. M. L. & Nicholson, L. J. Cancer stem cells: in the line of fire. *Cancer Treat. Rev.* **38**, 589–598 (2012).
20. Aktipis, C. A. et al. Cancer across the tree of life: cooperation and cheating in multicellularity. *Philos. Trans. R. Soc. Lond. B. Biol. Sci.* **370**, 20140219 (2015).
21. Velicer, G. J., Kroos, L. & Lenski, R. E. Developmental cheating in the social bacterium Myxococcus xanthus. *Nature* **404**, 598–601 (2000).
22. Davila, A. F. & Zamorano, P. Mitochondria and the evolutionary roots of cancer. *Phys. Biol.* **10**, 026008 (2013).
23. Thomas, F. et al. Evolutionary ecology of organs: a missing link in cancer development?. *Trends Cancer* **2**, 409–415 (2016).
24. Strand, S. et al. Lymphocyte apoptosis induced by CD95 (APO–1/Fas) ligand–expressing tumor cells — A mechanism of immune evasion?. *Nat. Med.* **2**, 1361–1366 (1996).
25. Ng, C. S., Novick, A. C., Tannenbaum, C. S., Bukowski, R. M. & Finke, J. H. Mechanisms of immune evasion by renal cell carcinoma: tumor-induced T-lymphocyte apoptosis and NFκB suppression. *Urology* **59**, 9–14 (2002).
26. Archetti, M. & Pienta, K. J. Cooperation among cancer cells: applying game theory to cancer. *Nat. Rev. Cancer* **19**, 110–117 (2019).
27. Van Valen, L. M. & Maiorana, V. C. HeLa, a new microbial species. *Evolut. Theor.* **10**, 71–74 (1991).
28. Sheridan, J. P. et al. Control of TRAIL-induced apoptosis by a family of signaling and decoy receptors. *Science* **277**, 818–821 (1997).
29. Pan, G. et al. The receptor for the cytotoxic ligand TRAIL. *Science* **276**, 111–113 (1997).
30. Wiley, S. R. et al. Identification and characterization of a new member of the TNF family that induces apoptosis. *Immunity* **3**, 673–682 (1995).
31. Rosenberg, H. M. Variant HeLa cells selected for their resistance to ouabain. *J. Cell. Physiol.* **85**, 135–142 (1975).
32. Kanalas, J. J., Hutton, J. J. & Suttle, D. P. Characterization of pyrazofurin-resistant HeLa cells with amplification of UMP synthase gene. *Somat. Cell. Mol. Genet.* **11**, 359–369 (1985).
33. Lin, Y.-C. et al. Genome dynamics of the human embryonic kidney 293 lineage in response to cell biology manipulations. *Nat. Commun.* **5**, 4767 (2014).
34. Good, B. H., McDonald, M. J., Barrick, J. E., Lenski, R. E. & Desai, M. M. The dynamics of molecular evolution over 60,000 generations. *Nature* **551**, 45–50 (2017).
35. Lenski, R. E., Rose, M. R., Simpson, S. C. & Tadler, S. C. Long-term experimental evolution in *Escherichia coli*. I. Adaptation and divergence during 2,000 generations. *Am. Nat.* **138**, 1315–1341 (1991).
36. Lenski, R. E. & Travisano, M. Dynamics of adaptation and diversification: a 10,000-generation experiment with bacterial populations. *Proc. Natl. Acad. Sci.* **91**, 6808–6814 (1994).
37. Blount, Z. D., Barrick, J. E., Davidson, C. J. & Lenski, R. E. Genomic analysis of a key innovation in an experimental Escherichia coli population. *Nature* **489**, 513–518 (2012).
38. Tenaillon, O. et al. Tempo and mode of genome evolution in a 50,000-generation experiment. *Nature* **536**, 165–170 (2016).
39. Callaway, E. Deal done over HeLa cell line. *Nature* **500**, 132–133 (2013).
40. Adey, A. et al. The haplotype-resolved genome and epigenome of the aneuploid HeLa cancer cell line. *Nature* **500**, 207–211 (2013).
41. Lazo, P. A., DiPaolo, J. A. & Popescu, N. C. Amplification of the integrated viral transforming genes of human papillomavirus 18 and its 5'-flanking cellular sequence located near the myc protooncogene in HeLa cells. *Cancer Res.* **49**, 4305–4310 (1989).
42. Macville, M. et al. Comprehensive and definitive molecular cytogenetic characterization of HeLa cells by spectral karyotyping. *Cancer Res.* **59**, 141–150 (1999).
43. Landry, J. J. M. et al. The genomic and transcriptomic landscape of a HeLa cell line. *G3 (Bethesda)* **3**, 1213–1224 (2013).
44. Bylund, L., Kytölä, S., Lui, W.-O., Larsson, C. & Weber, G. Analysis of the cytogenetic stability of the human embryonal kidney cell line 293 by cytogenetic and STR profiling approaches. *Cytogenet. Genome. Res.* **106**, 28–32 (2004).
45. Duan, G. et al. A Strategy to delay the development of cisplatin resistance by maintaining a certain amount of cisplatin-sensitive cells. *Sci. Rep.* **7**, 432 (2017).
46. Zhang, Y. et al. Genetic load and potential mutational meltdown in cancer cell populations. *Mol. Biol. Evol.* **36**, 541–552 (2019).
47. Hegreness, M., Shoresh, N., Hartl, D. & Kishony, R. An equivalence principle for the incorporation of favorable mutations in asexual populations. *Science* **311**, 1615–1617 (2006).
48. Velicer, G. J., Kroos, L. & Lenski, R. E. Loss of social behaviors by Myxococcus xanthus during evolution in an unstructured habitat. *Proc. Natl. Acad. Sci.* **95**, 12376–12380 (1998).
49. Wahl, L. M., Gerrish, P. J. & Saika-Voivod, I. Evaluating the impact of population bottlenecks in experimental evolution. *Genetics* **162**, 961–971 (2002).
50. Burch, C. L. & Chao, L. Evolution by small steps and rugged landscapes in the RNA virus ϕ6. *Genetics* **151**, 921–927 (1999).
51. Castello, A. et al. Insights into RNA biology from an atlas of mammalian mRNA-binding proteins. *Cell* **149**, 1393–1406 (2012).
52. Szczesny, R. J. et al. Versatile approach for functional analysis of human proteins and efficient stable cell line generation using FLP-mediated recombination system. *PLOS ONE* **13**, e0194887 (2018).
53. Kafri, M., Metzl-Raz, E., Jona, G. & Barkai, N. The cost of protein production. *Cell Rep.* **14**, 22–31 (2016).
54. Breslow, D. K. et al. A comprehensive strategy enabling high-resolution functional analysis of the yeast genome. *Nat. Methods* **5**, 711–718 (2008).

55. Huang, Q. et al. Caspase 3–mediated stimulation of tumor cell repopulation during cancer radiotherapy. *Nat. Med.* **17**, 860–866 (2011).
56. Wiser, M. J., Ribeck, N. & Lenski, R. E. Long-Term dynamics of adaptation in asexual populations. *Science* **342**, 1364–1367 (2013).
57. Egeblad, M., Nakasone, E. S. & Werb, Z. Tumors as organs: complex tissues that interface with the entire organism. *Dev. Cell* **18**, 884–901 (2010).
58. Scadden, D. T. The stem-cell niche as an entity of action. *Nature* **441**, 1075–1079 (2006).
59. Williams, M. J. et al. Quantification of subclonal selection in cancer from bulk sequencing data. *Nat. Genet.* **50**, 895–903 (2018).
60. Chattopadhyay, S. et al. Evolutionary unpredictability in cancer model systems. *Sci. Rep.* **15**, 20334 (2025).
61. Noble, R. et al. Spatial structure governs the mode of tumour evolution. *Nat. Ecol. Evol.* **6**, 207–217 (2022).

Acknowledgments

The authors thank Professor Piotr Zielenkiewicz for helpful comments and Dr. Przemysław Surowiecki for assistance with figure preparation.

Author contributions

Conceptualization: E.S., J.B. and S.K.; Methodology: E.S., J.B., R.J.S., I.G. and S.K.; Investigation: A.T., E.S., I.G., K.K-K.; Formal analysis: S.K. and E.S; Visualization: E.S. and S.K.; Resources: R.J.S. and E.S.; Data curation: S.K. and E.S.; Writing – original draft: S.K. and E.S.; Writing – review and editing: S.K. and E.S.; Funding acquisition: S.K.; Supervision: S.K. and E.S.

Funding

This work was supported by the National Science Centre in Poland (2014/13/B/NZ8/04719; awarded to S.K.).

Declarations

Competing interests

The authors declare no competing interests.

Additional information

Supplementary Information The online version contains supplementary material available at https://doi.org/10.1038/s41598-026-58033-9.

Correspondence and requests for materials should be addressed to E.S. or S.K.